Journal of the Korean Association of Crystal Growth
Vol. 11, No. 5 (2001) 231-237

High density plasma etching of novel dielectric thin films: Ta_2O_5 and $(Ba,Sr)TiO_3$

Hyun Cho†

Department of Materials Engineering, Miryang National University Miryang 627-702, Korea

(Received August 16, 2001)

Abstract Etch rates up to 120 nm/min for Ta_2O_5 were achieved in both SF_6/Ar and Cl_2/Ar discharges. The effect of ultraviolet (UV) light illumination during ICP etching on Ta_2O_5 etch rate in those plasma chemistries was examined and UV illumination was found to produce significant enhancements in Ta_2O_5 etch rates most likely due to photoassisted desorption of the etch products. The effects of ion flux, ion energy, and plasma composition on $(Ba,Sr)TiO_3$ etch rate were examined and maximum etch rate ~90 nm/min was achieved in Cl_2/Ar ICP discharges while $CH_4/H_2/Ar$ chemistry produced extremely low etch rates (≤ 10 nm/min) under all conditions.

Key words High density plasma etching, Dielectric thin film, Ta_2O_5, $(Ba,Sr)TiO_3$, ICP etching, UV illumination

1. Introduction

There has been extensive effort over the past decade to develop novel dielectric thin films which can be a replacement for SiO_2 and the leading candidates are Ta_2O_5 and $(Ba,Sr)TiO_3$ based on their high dielectric constant (Ta_2O_5 : 25~35, $(Ba,Sr)TiO_3$: 200~500), low leakage current and high breakdown voltage characteristics [1-3]. These films have many application fields include a dielectric layer for storage capacitors in dynamic random access memory (DRAM) and gate insulators in metal oxide field effect transistors (MOSFET) [4-5]. Recently, Ta_2O_5 has found new application fields as an etch mask during surface or bulk micromachining of Si, as an insulating layer in thin film electroluminescent display devices, and as a detection layer in biological and chemical sensors [6-8]. However, relatively little work has been done on dry etching of these thin films, which is preferred method of forming small structures due to the difficulty in wet etching while dry etching process for conventional SiO_2-based dielectric structures are well-developed. Previous reports have found relatively low etch rates for Ta_2O_5 in fluorocarbon-based plasma chemistries such as CF_4, C_2F_6, CHF_3 and CF_3Cl [9]. There have been two basic classes of electrode materials employed to date, namely, those based on elemental metals, predominantly Pt or those based on metallic oxides such as IrO_2, RuO_2, and high T_c superconductors [10]. The metallic oxides have a potential advantage in improving the fatigue performance of capacitors. In this work, $LaNiO_3$ was chosen as the metallic oxide for use with $(Ba,Sr)TiO_3$ films, since is displays several advantages as an electrode material [11-13].

In this paper we report on high density plasma etching of Ta_2O_5 and $(Ba,Sr)TiO_3$ thin films in a variety of different plasma chemistries, namely SF_6/Ar, SF_6/O_2, Cl_2/Ar, and $CH_4/H_2/Ar$, and the significant enhancement in Ta_2O_5 etch rate by ultraviolet (UV) light illumination during inductively coupled plasma (ICP) etching.

2. Experimental

Around 100 nm thick amorphous Ta_2O_5 and 200~300 nm thick polycrystalline $(Ba,Sr)TiO_3$ films were deposited on (100) Si substrates by either plasma enhanced chemical vapor deposition (PECVD) at 350°C or pulsed laser deposition (PLD, KrF excimer laser, 5 Hz pulse frequency) at 650°C. The precursors used for Ta_2O_5 were $Ta(C_2H_5O_5)$ and O_2 with total flow rates of 200 standard cubic centimeters per minute (sccm) and pressed powder targets were used for $(Ba,Sr)TiO_3$ deposition.

The samples were patterned with either Apiezon wax or photoresist and were etched in a Plasma-Therm ICP 790 reactor. The plasma is sustained in a three-turn, cylindrical geometry source operating at 2

†Corresponding author
Tel: 82-55-350-5456
Fax: 82-55-353-5457
E-mail: hcho@arang.miryang.ac.kr

MHz and powers up to 1000 W. The samples were thermally bonded to a Si carrier wafer on He back-side cooled, rf powered (13.56 MHz) chuck, at powers up to 350 W. The process pressure was held at 2~5 mTorr and gas loading into the source was controlled through mass flow controllers at a typical load of 15~20 sccm. For UV illumination during ICP etching, a Hg arc lamp (400 W) was installed on 1 in. diameter quartz window on top of the ICP source, ~20 cm from the sample position, and sample heating due to the UV illumination is minimal (< 10°C). The etch depths were examined by TENCOR stylus profilometry measurements after the removal of the mask, and used to calculate the etch rates. The error in these measurements is approximately ±10 %. The surface morphology and surface roughness of selected samples were examined with Atomic Force Microscopy (AFM, Digital Instrument Nanoscope III) using a Si tip in tapping mode. The selectivity of etch was calculated for Si over Ta_2O_5.

3. Results and Discussion

3.1. ICP etching of Ta_2O_5

Figure 1 shows a comparison of Ta_2O_5 and Si etch rates, with the resultant selectivities, as a function of discharge composition in SF_6/Ar (left) and SF_6/O_2 (right). The etch rates for Ta_2O_5 increase more slowly with increasing SF_6 concentration than do the rates for Si, with the consequence that the maximum selectivity for Si over Ta_2O_5 is achieved in pure SF_6 discharges. The dc self-bias increases in both chemistries as the SF_6 concentration increases, indicating that the positive ion density is decreasing. Note that Ta_2O_5 etch

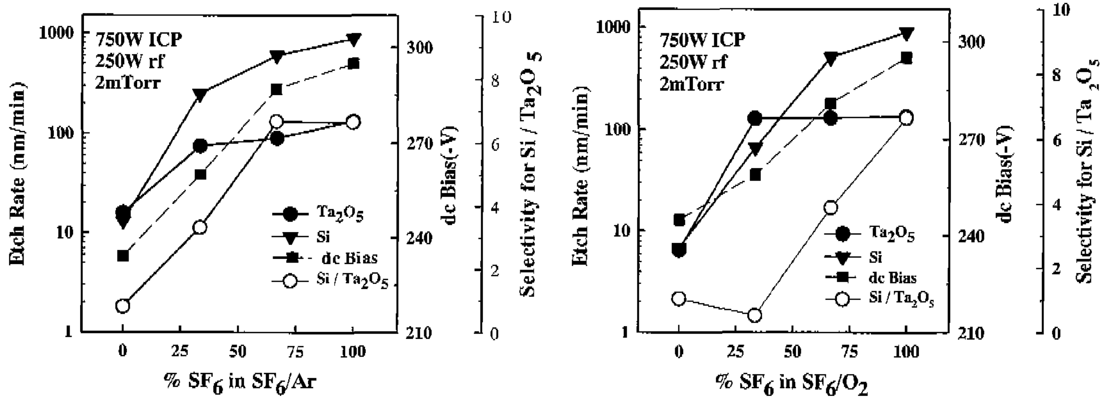

Fig. 1. Etch rates and selectivities for Si over Ta_2O_5 in SF_6/Ar (left) and SF_6/O_2 (right) ICP discharges (750 W source power, 250 W rf chuck power, 2 mTorr), as a function of SF_6 concentration.

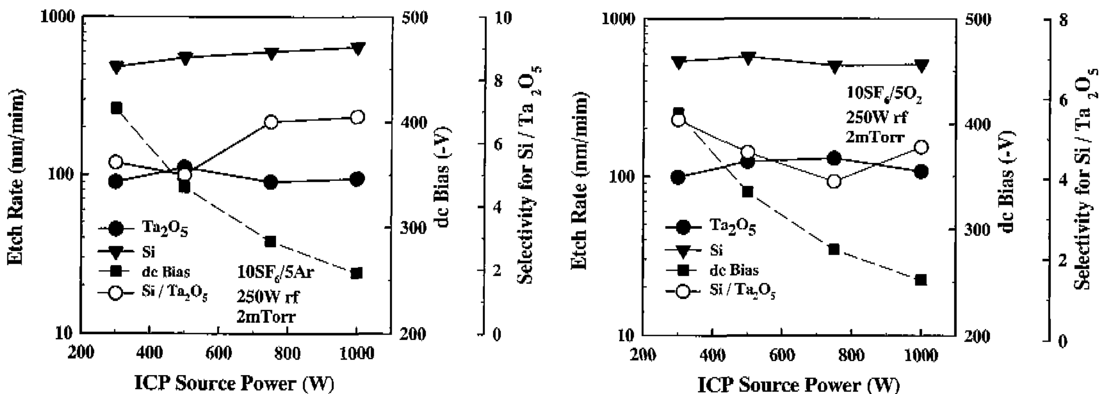

Fig. 2. Etch rates and selectivities for Si over Ta_2O_5 in $10SF_6/5Ar$ (left) and $10SF_6/5O_2$ (right) ICP discharges (250 W rf chuck power, 2 mTorr), as a function of ICP source power.

rates of ~20 nm/min are achieved in the SF_6-based mixtures, at dc self-biases in the range of 215 to 290 V. We could not detect the etch products for Ta_2O_5 with optical emission spectroscopy (OES), but assume they are probably TaF_x and O_2. In the case of Si, we readily observed the SiF_x etch products, with emission lines in the range of 400~430 nm.

The effect of ICP source power on the Ta_2O_5 etch rates is shown in Fig. 2 for fixed plasma composition. The Si etch rate increases either modestly or not all over the range of 300~1000 W, while the Ta_2O_5 etch rate tends to decrease at the higher powers. This decrease is at least partially caused by the fall-off in dc self-bias, which is suppressed as the positive ion density in the discharge increases at higher powers. It is clear that because Si etches in atomic fluorine even without ion bombardment, whereas Ta_2O_5 does not, there will always be a faster etch rate for Si in non-polymer-forming plasma chemistries.

In high density plasma etching the rf chuck power controls the incident ion energy approximately equal to the sum of the plasma potential (roughly 25 V in this tool, from Langmuir probe measurements) and the dc self-bias. It is expected an increase in rf chuck power increases the etch rates of both Ta_2O_5 and Si because of the improved efficiency of ion-assisted reactions. Figure 3 shows the trend consistent with this expectation for both SF_6/Ar and SF_6/O_2. Selectivity for Si over Ta_2O_5 is found to decrease with increasing ion energy because of the larger contribution of physical process relative to chemical component of the etching.

The surface morphologies of the etched Ta_2O_5 were examined by AFM and Fig. 4 shows the measured root-mean-square (RMS) roughness measured over 1 mm^2 area after exposure to SF_6/Ar or SF_6/O_2 discharges. The Ta_2O_5 surface roughness values are unchanged from the unetched control values, whereas the Si shows some etch-induced texture structure on the surfaces. In each case the etch was performed for 30 secs corresponding to etch depths of ~45 nm for Ta_2O_5 and ~250 nm for Si.

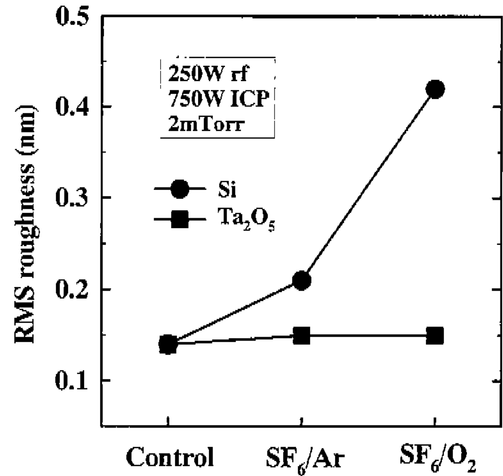

Fig. 4. RMS roughness values of Ta_2O_5 and Si surfaces before and after etching in $10SF_6/5Ar$ and $10SF_6/5O_2$ ICP discharges (750 W source power, 250 W rf chuck power, 2 mTorr).

Figure 5 shows the effects of source power (left) and rf chuck power (right) on the Ta_2O_5 and Si etch rates at fixed plasma composition ($10Cl_2/5Ar$). The etch rates for both materials decrease at high values of either parameter, a trend often observed in high density plasma etching and often ascribed to ion-

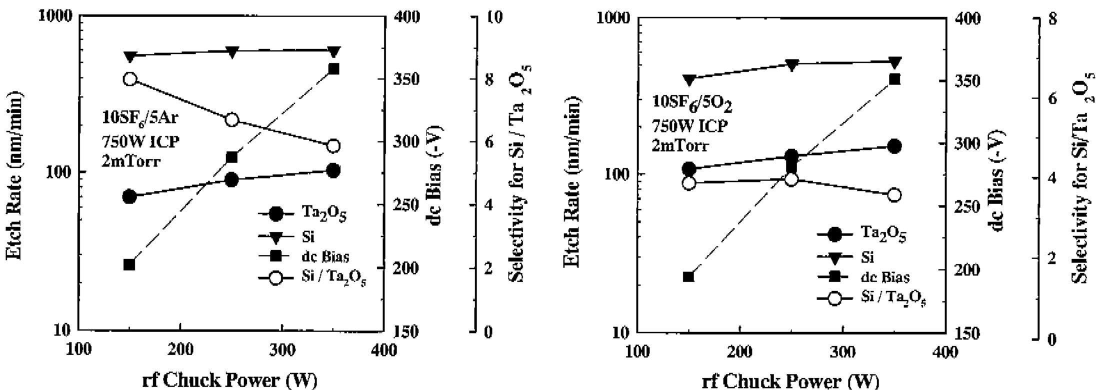

Fig. 3. Etch rates and selectivities for Si over Ta_2O_5 in $10SF_6/5Ar$ (left) and $10SF_6/5O_2$ (right) ICP discharges (750 W source power, 2 mTorr), as a function of rf chuck power.

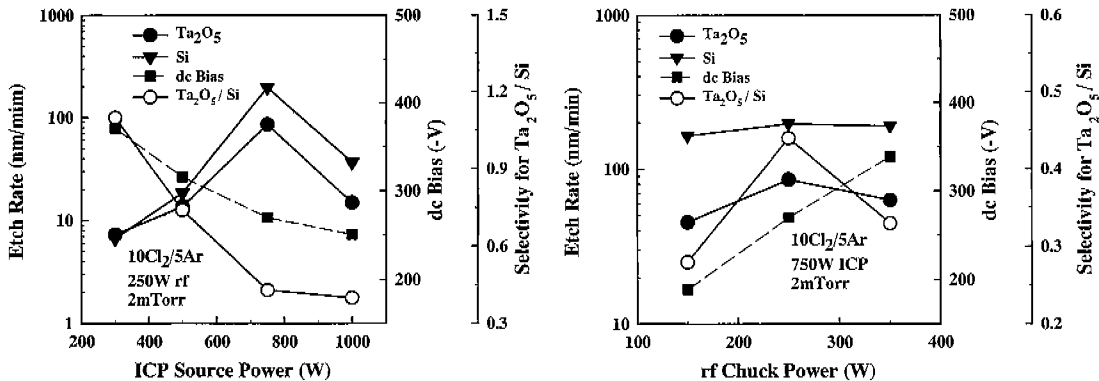

Fig. 5. Etch rates and selectivities for Ta_2O_5 over Si in $10Cl_2/5Ar$ ICP discharges as a function of source power (left) or rf chuck power (right).

assisted desorption of the reactive neutrals before they can react with the substrate [14]. The Ta_2O_5/Si selectivities again fall in the range of 0.3-1 over the whole range of conditions investigated.

3.2. *The UV light enhancement of Ta_2O_5 dry etch rates*

Figure 6 shows the Ta_2O_5 etch rates in $10SF_6/5Ar$ discharges as a function of ICP source power (left) and rf chuck power (right). At the low chuck power condition (100 W) the etch rate enhancement with UV illumination increases with source power and reaches a factor of approximately 2 in the range of 500~750 W. By sharp contrast, at higher rf chuck power conditions (Fig. 6, right) there is essentially no increase in etch rate as a result of UV illumination. At higher ion energies the etch rates decrease both with and without UV illumination due to the ion-assisted removal of the reactive neutrals [14]. Several groups have reported that UV irradiation during dry etching dramatically enhances the etch rate of Cu in Cl_2-based high density plasmas, through transforming involatile $CuCl_x$ etch products into more volatile species (e.g. Cu_2Cl_3) and subsequent non-thermal desorption of these species. [15] In the case of Ta_2O_5, an analogous situation would involve photodesorption of TaF_x species since the oxygen should be removed as O_2 or oxyfluorides.

In the case of Cl_2/Ar discharges, Fig. 7 shows that UV illumination did lead to faster Ta_2O_5 etch rates at moderate source power (left) and rf chuck powers (right). This seems plausible from the following scenarios- at very high ion fluxes or energies, the $TaCl_x$ etch product is being efficiently removed by sputter-assisted desorption whether or not the UV illumina-

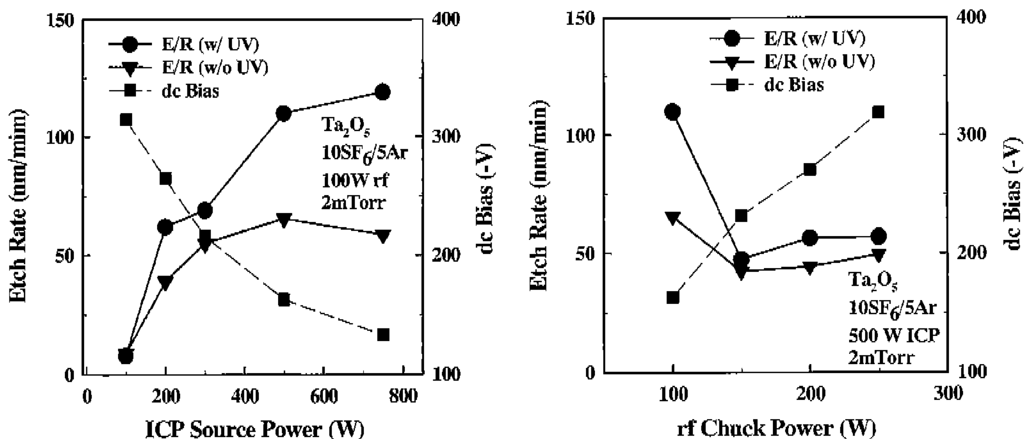

Fig. 6. Ta_2O_5 etch rates with and without UV illumination in $10SF_6/5Ar$ ICP discharges as a function of source power (left) or rf chuck power (right).

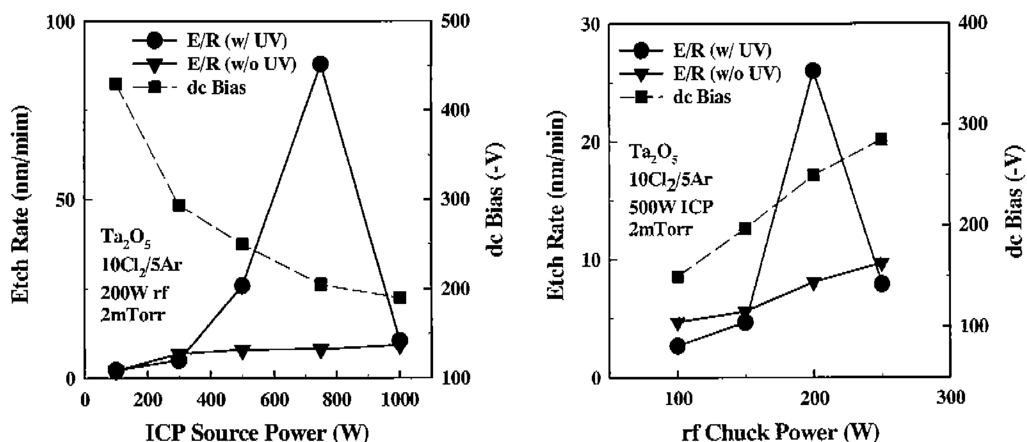

Fig. 7. Ta_2O_5 etch rates with and without UV illumination in $10Cl_2/5Ar$ ICP discharges as a function of source power (left) or rf chuck power (right).

tion is being used, whereas at very low ion fluxes or energies the etch rate may be controlled by diffusion of the etch products through a chlorinated selvedge layer. For the Cl_2-based plasma chemistry the physical process dominates the etch process and UV illumination is less important over a broad range of conditions than with SF_6 plasma chemistry.

3.3. *ICP etching of (Ba,Sr)TiO$_3$*

Figure 8 shows the rf chuck power dependence of $(Ba,Sr)TiO_3$ and $LaNiO_3$ etch rates in $10Cl_2/5Ar$ (left) or $5CH_4/10H_2/5Ar$ (right) discharges at fixed source power (750 W) and pressure (2 mTorr). In $10Cl_2/5Ar$ discharges, the etch rate of $(Ba,Sr)TiO_3$ increases with the higher ion bombardment energy up to approximately 250 W rf chuck power and decreases thereafter. This trend is again, as mentioned earlier, ascribed to ion-assisted desorption of the adsorbed chlorine neutral before the etch products are formed on the surface. In the case of $LaNiO_3$ we do not observe the decrease in etch rate at higher rf chuck powers, suggesting the amount or stability of the adsorbed chlorine is different than for $(Ba,Sr)TiO_3$. By sharp contrast, extremely low etch rates (≤ 10 nm) were obtained for both $(Ba,Sr)TiO_3$ and $LaNiO_3$ in $5CH_4/10H_2/5Ar$ discharges and the etching is dominated by the physical sputtering since there is no apparent chemical contribution to the etching, with the results similar to those obtained with pure Ar plasmas.

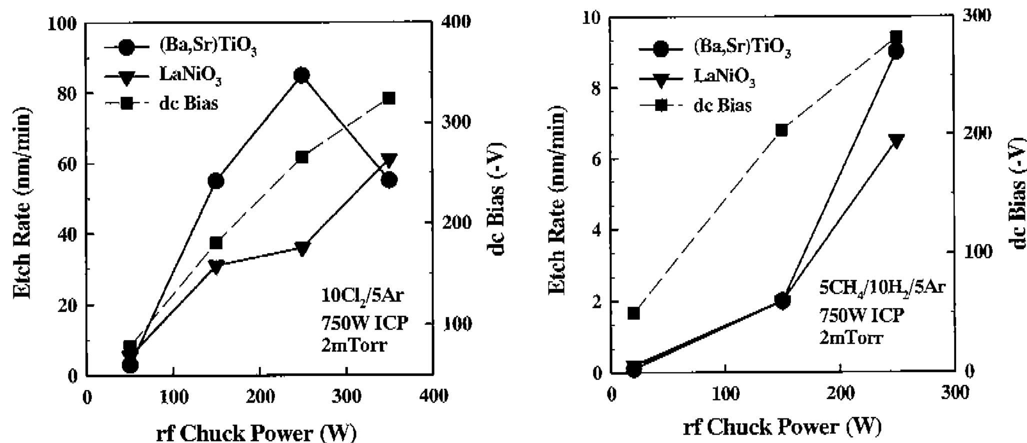

Fig. 8. Etch rates for $(Ba,Sr)TiO_3$ and $LaNiO_3$ in $10Cl_2/5Ar$ (left) or $5CH_4/10H_2/5Ar$ (right) ICP discharges (750 W source power, 2 mTorr) as a function of rf chuck power.

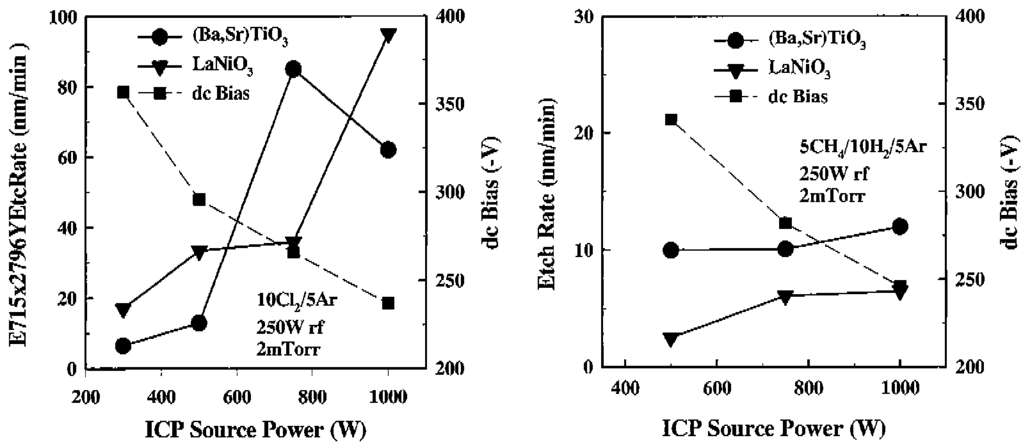

Fig. 9. Etch rates for $(Ba,Sr)TiO_3$ and $LaNiO_3$ in $10Cl_2/5Ar$ (left) or $5CH_4/10H_2/5Ar$ (right) ICP discharges (250 W rf chuck power, 2 mTorr) as a function of source power.

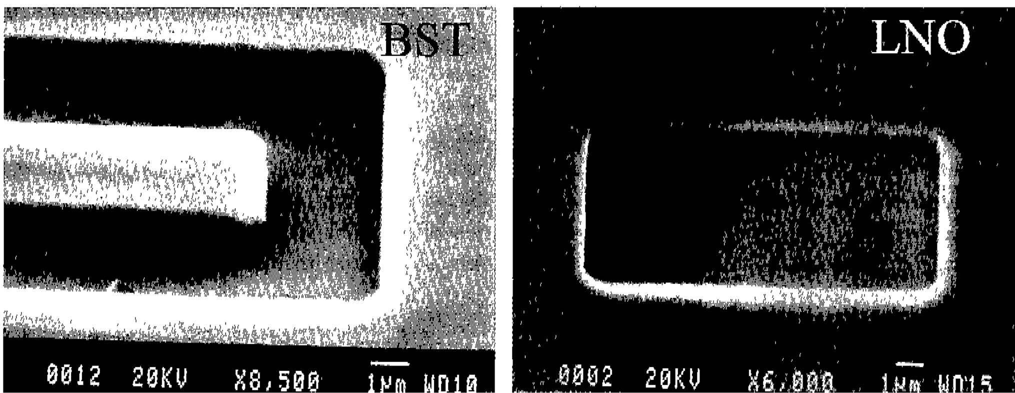

Fig. 10. SEM micrographs of features etched into $(Ba,Sr)TiO_3$ (left) and $LaNiO_3$ (right) using $10Cl_2/5Ar$ ICP discharges (750 W source power, 250 W rf chuck power, 5 mTorr).

The influence of ICP source power on the etch rates of both $(Ba,Sr)TiO_3$ and $LaNiO_3$ in $10Cl_2/Ar$ (left) or $5CH_4/10H_2/5Ar$ (right) discharges at fixed rf chuck power (250 W) and pressure (2 mTorr) is shown in Fig. 9. In high density plasma etching, increasing the source power suppresses the dc self-bias because of the higher conductivity of the plasma and this leads to two competing effects, namely an increase in ion flux but a decrease in ion energy. This competition is reflected in an initial increase in $(Ba,Sr)TiO_3$ etch rate in $10Cl_2/5Ar$ mixtures, followed by a decrease when the dc self-bias falls below approximately 270 V. Once again the $LaNiO_3$ etch rate shows different behavior, with a continuing increase in etch rate over the range of source powers we investigated. $5CH_4/10H_2/5Ar$ mixtures again produced low etch rates for both materials under all conditions most likely due to the deposition of a polymer layer from the CH_4, which may act to shield the surface from the ion bombardments.

Since high density plasma etching for $(Ba,Sr)TiO_3$ and $LaNiO_3$ in $10Cl_2/5Ar$ discharges is ion-driven etching under all conditions investigated, highly anisotropic features can be formed with a minimized mask erosion, and SEM micrographs of the features etched into $(Ba,Sr)TiO_3$ (left) and $LaNiO_3$ (right) are shown in Fig. 10. A 7 μm thick photoresist mask was used as a mask material and about one-third of the resist remained at the completion of the etching.

4. Conclusions

A number of different inductively coupled plasma chemistries (SF_6/O_2, SF_6/Ar and Cl_2/Ar) were examined

for dry etching of Ta_2O_5 and maximum etch rates ~120 nm/min were achieved in fluorine- or chlorine-based mixtures. The etch selectivities for Si over Ta_2O_5 of ~6 were achieved in SF_6 ICP discharges since Ta_2O_5 etch rates were always slower than those of Si and the reverse selectivity was not achieved.

The UV illumination during ICP etching of Ta_2O_5 in both SF_6/Ar and Cl_2/Ar plasma chemistries produces significant enhancements in etch rates. The increased etch rates are likely due to photoassisted desorption of the TaF_x and $TaCl_x$ etch products. The use of UV illumination is an alternative to employing elevated temperatures during etching to increase the volatility of the etch products and may find application where the thermal budget should be minimized during processing.

Two common semiconductor plasma chemistries, namely Cl_2/Ar and $CH_4/H_2/Ar$, have been examined for dry etching of thin films of $(Ba,Sr)TiO_3$ and $LaNiO_3$. The etching in both chemistries is physically dominated, but only Cl_2/Ar produces reasonable etch rates, and smooth and anisotrpic pattern transfer was performed.

References

[1] B.C. Lai and J.Y. Lee, Leakage Current Mechanism of Metal-Ta_2O_5-metal Capacitors for Memory Device Applications, J. Electrochem. Soc. 146 (1999) 266.

[2] K.W. Kwon, C.S. Kang, S.O. Park, H.K. Kang and S.T. Ahn, Thermally Robust Ta_2O_5 Capacitor for the 256-Mbit DRAM, IEEE Trans. Electron. Dev. 43 (1996) 919.

[3] S.O. Kim and H.J. Kim, Fabrication of n-metal-oxide Semiconductor Field Effect Transistor with Ta_2O_5 Gate Oxide Prepared by Plasma Enhanced Metalorganic Chemical Vapor Deposition, J. Vac. Sci. Technol. B 12 (1994) 3006.

[4] H. Shimada and T. Ohmi, Current Drive Enhancement by Using High-permittivity Gate Insulator in SOI MOSFET's and its Limitation, IEEE Trans. Electron. Dev. 43 (1996) 431.

[5] K. Kukli, J. Ihances, M. Ritala and M. Leskela, Properties of Ta_2O_5-based Dielectric Nanolaminates Deposited by Atomic Layer Epitaxy, J. Electrochem. Soc. 144 (1997) 300.

[6] A.K. Chu, Y.S. Huang and S.H. Tang, Room-temperature Radio Frequency Sputtered Ta_2O_5 : A New Etch Mask for Bulk Silicon Dissolved Processes, J. Vac. Sci. Technol. B 17 (1999) 455.

[7] K. Kukli, J. Ihances, M. Ritala and M. Leskela, Tailoring the Dielectric Properties of HfO_2-Ta_2O_5 nanolaminates, Appl. Phys. Lett. 68 (1996) 3737.

[8] Y. Kuo, Reactive Ion Etching of Sputter Deposited Tantalum Oxide and its Etch Selectivity to Tantalum, J. Electrochem. Soc. 139 (1992) 579.

[9] S. Seki, T. Unagami, and B. Tsujiyama, Reactive Ion Etching of Tantalum Pentoxide, J. Electrochem. Soc. 130 (1983) 2505.

[10] S.M. Hong, S.M. Rhim, H.J. Bak and O.K. Kim, Deposition Characteristics of $(Ba,Sr)RuO_3$ Thin Films Prepared by Ultrasonic Spraying Deposition, J. Kor. Assoc. Crystal Growth 11 (2001) 111.

[11] C.R. Cho, D.A. Payne and S.L. Cho, Solution Deposition and Heteroepitaxial Crystallization of $LaNiO_3$ Electrodes for Integrated Ferroelectric Devices, Appl. Phys. Lett. 71 (1997) 3013

[12] M.S. Chen, T.B. Wu and J.-M. Wu, Effect of Textured $LaNiO_3$ Electrode on the Fatigue Improvement of $Pb(Zr_{0.53}Ti_{0.47})O_3$ Thin Films, Appl. Phys. Lett. 68 (1996) 1430.

[13] A. Li, C. Be, P. Lu, D. Wu, S. Xing and N. Ming, Fabrication and Electrical Properties of Sol-gel Derived $BaTiO_3$ Films with Metallic $LaNiO_3$ Electrode, Appl. Phys. Lett. 70 (1997) 1616.

[14] R.J. Shul, G.B. McClellan, R.D. Briggs, D. Rieger, S.J. Pearton, C.R. Abernathy, J.W. Lee, C. Constantine and C. Barrat, High-density Plasma Etching of Compound Semiconductors, J. Vac. Sci. Technol. A 15 (1997) 633.

[15] K.-S. Choi and C.-H. Han, Low Temperature Copper Etching Using an Inductively Coupled Plasma with Ultraviolet Light Irradiation, J. Electrochem. Soc. 145 (1998) L37.